Journal of
NANOSTRUCTURES
JNS
NANOSTRUCTURES
JNS.kashanu.ac.ir

Magnetic Properties of $Fe_{49}Co_{33}Ni_{18}$Nanowire ArraysStudied by First-Order Reversal Curve Diagrams

S. Samanifar[a,*],M. AlmasiKashi[a,b], A. Ramazani[a,b]

[a]*Department of Physics, University of Kashan, Kashan, 87317-51167, Iran*

[b] *Institute of Nanoscience& Nanotechnology, University of Kashan, Kashan, 87317-51167, Iran*

Article history:
Received 15/10/2014
Accepted 16/11/2014
Published online 21/12/2014

Keywords:
FeCoNi nanowires
FORC diagrams
Pulsed ac electrodeposition
Magnetostatic interactions

**Corresponding author:*
E-mail address:samanifar@grad.kashanu.ac.ir
Phone: +98 3615552935
Fax: +98 3615552935

Abstract

$Fe_{49}Co_{33}Ni_{18}$ nanowire arrays (175 nm in diameter and lengths ranging from 5 to 32μm) were fabricated into nanopores of hard-anodized aluminum oxide templates using pulsed ac electrodeposition technique. Hysteresis loop measurements indicated that increasing the length decreases coercivity and squareness values (from 274 Oe and 0.58 to200 Oe and 0.105, respectively), indicating the increase in magnetostatic interactions between the nanowires (NWs).On the other hand, first-order reversal curve measurements showed a linear correlation between the magnetostatic interactions and length of NWs. It was also found that with increasing length, the domain structure of NWs changed from single-domain to pseudo single-domain state. A multidomain-like behavior is also seen for the longest NWs length.Increasing the length of NWs resulted in an increase inthe interaction and decrease in the array coercive field(H_c^{Array}) as beingsmaller than that of individual NWs (H_c^{FORC}).The observed CFD component in the FORC diagrams of FeCoNi NWs with shorter lengths was a consequence ofnon-uniform length distributions.

1. Introduction

Nanostructured magnetic materials have been the subject of a lot of growth in order to understand their remarkable magnetic properties. In this respect, magnetic nanowires (NWs) address both important fundamental and application aspects. Their small size and tunable properties make them

appropriate to be used for minimizing conventional devices in applied areas such as optics, electronics, spintronics, sensors, magnetic storage devices and thermoelectric [1-3]. Among the different fabrication methods of magnetic nanowire arrays, the electrodeposition into anodic aluminum oxide (AAO) template as a simple, cheap, and effective method is widely used to control the length and the diameter of wires as well as interwire distance through controlling anodizationparameters [4]. Arrays of magnetic NWs with high crystallinity, large aspect ratio and high length uniformity can be obtained by controlling the electrodepositionparameters [5-7].

Magnetostatic interactions between magnetic elements are one of the major determinants of signal-to-noise ratio and are responsible for data loss in magnetic recording media [8,9]. Therefore, it is important to have a reliable method for measuring magnetic interactions in magnetic systems. The greater interpore distances and lower degree of porosity of hard anodized anodic aluminum oxide (HA-AAO) template than for mild anodized anodic aluminum oxide (MA–AAO) allows to probe magnetostatic interactions between magnetic wires in wider range of interwiredistances [4, 10, 11].

The isothermal remanent magnetization (IRM) [12], DC demagnetization remanence (DCD) [13] curves and δM curves[14] are conventional methods to characterize magnetic interactions. The first-order reversal curve (FORC) diagrams as an efficient experimental tool have been recently proposed to study highly interacting systems, like ferromagnetic nanowire arrays [15,16]. The FORC diagrams as a powerful method, give details of magnetic interactions, coercivity distribution and behavior of domains formed in a material (SD, MD, PSD and superparamagnetic (SP)) [17, 18]. To plot a FORC, the sample is saturated by a positive applied field. The field is then decreased to a reversal H_r field which is always less than H_{max}. The magnetization $M(H,H_r)$ is measured in each step until $H_r \geq -H_{max}$. A FORC distribution is defined as the mixed second derivative:

$$\rho(H_r,H) = -\frac{1}{2}\frac{\partial^2 M(H_r,H)}{\partial H_r \partial H} \quad (1)$$

which is well defined for $H>H_r$.

A FORC diagram is a contour plot of $\rho(H, H_r)$ along 45°-rotated axes ($H_c = (H - H_r)/2$, $H_u = H + H_r)/2$). The $\rho(H, H_r)$ at a point is calculated by fitting a polynomial surface $a_1 + a_2H + a_3H^2 + a_4H_r + a_5 H_r^2 + a_6HH_r$ over a local grid centered on the point. The $\rho(H, H_r)$ at the center of the array can be estimated by a_6. $(2*SF+1)^2$ is known as a number of the fitted data points, in which SF is smoothing factor [18]. An increase in SF decreases the contribution of noise and increases the smoothness of the FORC diagram.

SD diagrams are characterized by closed contours extending along the H_c axis and with vertical spread along the H_u axis [18]. PSD systems show a closed-contour distribution that is more spread out along the horizontal axis, with a peak moving toward the H_u axis [19]. For MD stats, the contours are broaden along the H_u axis and ultimately form vertical contours [20]. The presence of interactions usually produces a spreading of the distribution in the vertical direction of a FORC diagram [21].

Recently, FORC diagrams of different NWs have been studied. Ivanvo et al. observed that magnetostatic interactions between hexagonal close packed Co NWs in an array result in a reduction of coercivity and squarenessvalues [22]. According to Béron et al., increasing the length of Ni and CoFeB nanowire arrays does not change

their initial SD structure. Moreover, with increase of the length, maximum coercive fields of out-of-plane FORC diagrams linearly decrease with increase of interaction fields [23].

In the present work, FeCoNi NWs have been grown into the nanopores of HA-AAO template by ac pulse electrodeposition technique. The aim of this work is the study of the influence of magnetostatic interactions on the magnetic properties of FeCoNi nanowire arrays with different lengths. To demonstrate this effect, FeCoNiNWs with various lengths were electrodeposited by changing deposition time. Composition and crystalline characteristics of the NWs with different lengths are carried out. After eliminating the dendrites formed at the pores' bottom, magnetic behavior of nanowire arrays as a function of wire length were investigated by hysteresis loop measurements. Coercivity distribution and magnetostatic interactions between the NWs with different lengths were studied based on FORC diagrams.

2. Experimental procedure

High purity (99.999%) aluminum foils with 10 mm diameter and 0.3 mm thickness were ultrasonically cleaned in acetone. The samples were electropolished in a 1:4 volume mixture of perchloric acid and ethanol for 3 min under a current density of 100 mA/cm^2 and washed with deionized water. The samples were then anodized at 40 V for 5 min in 0.3 M oxalic acid solution at 0°C. The Anodization voltage was increased to 130 V at a rate of 0.5 V/s, where it kept constant for 90 min to obtain long nanopores. To thin the barrier layer formed during the hard regime, the voltage was exponentially decreased from 130 to 40 V at 17°C.

The diameter of prepared nanopores was then enlarged by etching treatment under 0.3 M phosphoric acid solution at 30°C for 100 min. Following the widening process, the samples were re- anodized at 40 V for 10 min at 17°C, and the voltage was then systematically reduced to 10 V to promote thinning of the barrier layer. To deposit ions into the pores, a bath consisting of 0.15 M $CoSO_4 \cdot 7H_2O$, 0.15 M $FeSO_4 \cdot 7H_2O$, 0.9 M $NiSO_4 \cdot 6H_2O$, 45 g/l boric acid and 1 g/l ascorbic acid was used. The electrolyte acidity was adjusted to 5 using $NaHCO_3$ solution. Electrodeposition process was performed with an initial reduction voltage of 11 V, constant oxidation voltage of 10 V, reduction/ oxidation time of 2.4/ 2.4 ms, and off-time of 96ms. During the process, the maximum reduction current density was kept constant at 40 mA/cm^2. The voltage and current density pulse related to the initial deposition time is shown in Fig. 1.

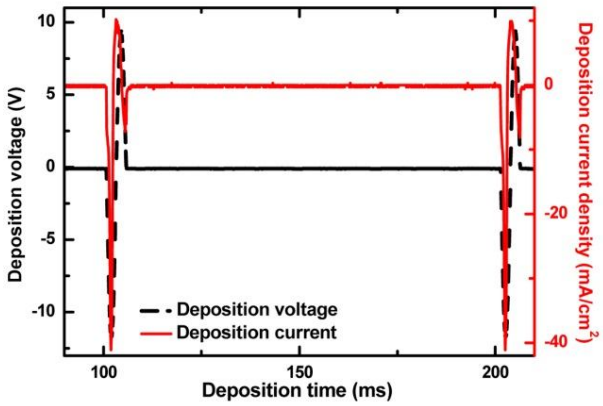

Fig. 1. The electrodeposition current density and ac pulse voltage with the reduction/oxidation time of 2.4 ms, off time of96msand maximum reduction current density of 40 mA/cm^2.

To explore the effect of length on the magnetic properties, a set of samples with various lengths were prepared by changing the deposition time. The dendrites were removed to eliminate their

effect on the magnetic properties of the samples, as reported elsewhere [24].

According to our previous work, it was possible to estimate the length of NWs by magnetic moment measurements [24]. In the present study, by fixing the surface area of the samples and changing only the electrodeposition time, FeCoNi NWs with four different lengths (32, 26, 14, 9 and 5μm) were fabricated. In this respect, the highest length was determined using scanning electron microscopy (SEM), while those of the rest of the lengths were estimated.

The composition and crystalline characteristic of FeCoNi nanowire arrays with different lengths were studied using electron dispersive spectroscopy (EDS)and X-ray diffraction (XRD). Magnetic measurements were then performed and hysteresis loop curves and FORC diagrams of the samples were plotted using a vibrating sample magnetometer (VSM) at room temperature.

3. Results and discussion

Cross-sectionalSEM images of 32μm long FeCoNi NWs after release and elimination of the dendritic NWs are shown in Fig. 2. As seen, the FeCoNi NWs with high degree of length uniformity behave as strongmagnets, attracted to each other.Moreover, since the etching rate of nanopores in 0.3 M acid phosphoric is estimated to be 1.25 nm/min [25], a 175 nm diameter was expected after etching treatment for 100 min.

Fig. 3 shows the XRD patterns of FeCoNi NWs with length of 32μm. As seen in our previous work, two distinct bcc FeCo and fccFeNi phases are observed so that the bcc phase is dominant, indicating the polycrystalline nature of the sample with a preferred orientation (i.e., FeCo(110)). Therefore, it can be said that there is no considerable change of microstructure for different lengths of FeCoNi NWs [24].

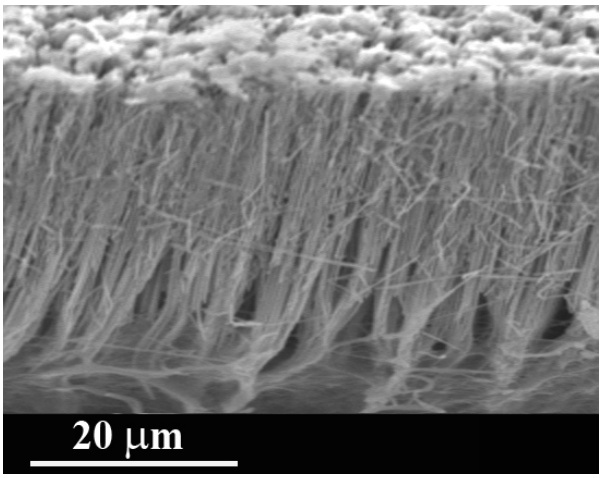

Fig.2. Cross-sectional SEM image of FeCoNi nanowire arrays with length of 32 μmafter release and elimination of dendritic NWs.

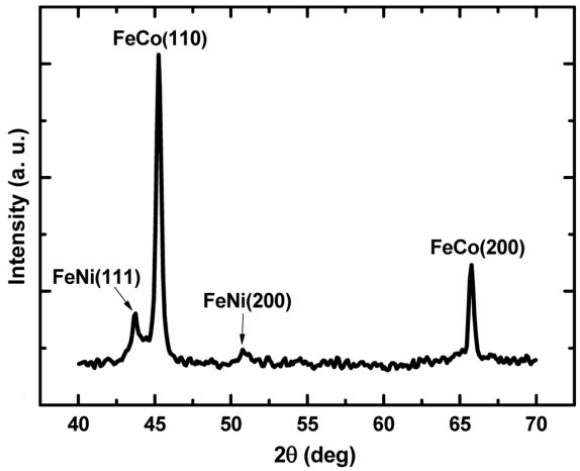

Fig. 3.XRD pattern of FeCoNi NWs with with length of 32 μm.

TheEDSmicroanalyses of FeCoNi nanowire arrays with lengths of32 and 14μmaretypically shownin Fig. 4 and theobtainedEDSresultsaretabulatedin Table1.It is seen that the composition is nearly constant to $Fe_{49}Co_{33}Ni_{18}$ and the composition of FeCoNi NWs does not considerably change as a function of length.

To explore the effect of length on the magnetic properties of NWs, magnetization measurements were carried out at room temperature with applied field parallel to the wires axis. Hysteresis loops show that increase in the length linearly increases saturation magnetic moment of the samples (Fig. 5(a)). The length dependence of saturation magnetic moment of FeCoNi nanowire arrays is inserted in Fig. 5(a). The coercivity and squareness as a function of length are shown in Fig. 5(b). As observed, increasing length from 5 to 32μm decreases the coercivity and squareness from 274Oe and 0.58 to 200Oe and 0.105, respectively.The enhancement of coercivity and squareness could be due to the decrease in magnetostatic interactions between the nanowire arrays.

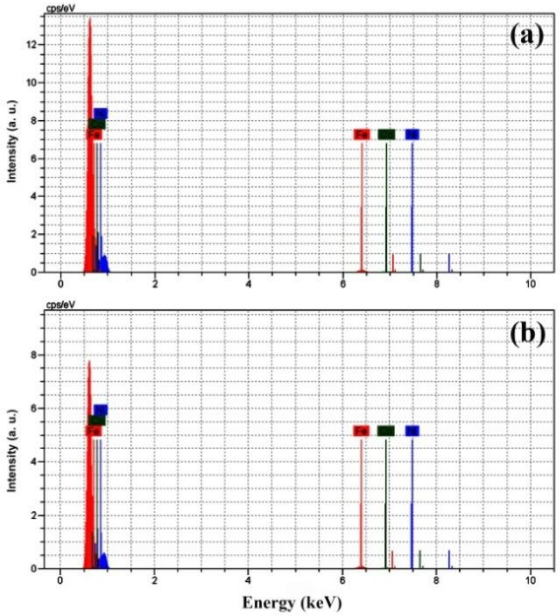

Fig. 4.EDS patterns of FeCoNi nanowire arrays with lengths of (a) 32 and (b) 14μm.

Table 1. Compositional characterization of FeCoNi nanowire arrays with lengths of 32 and 14μm.

Length	Fe	Co	Ni
(μm)	**[at. %]**	**[at. %]**	**at. %**
32	48.47	33.23	18.3
14	49.06	33.48	17.1

The shape anisotropy of the samples is the same since the aspect ratio is more than 10 [26], the crystalline anisotropy is also almost the same as shown in XRD pattern of Fig. 3. As mentioned above, the NWs composition does not considerably change with the length, therefore the Curie temperature remains almost constant and the exchange interactions would be the same for all samples [27]. Accordingly, it appears that, the magnetostatic interactions play a major role on the change in the magnetic properties of FeCoNi NWs with different lengths [28, 29].

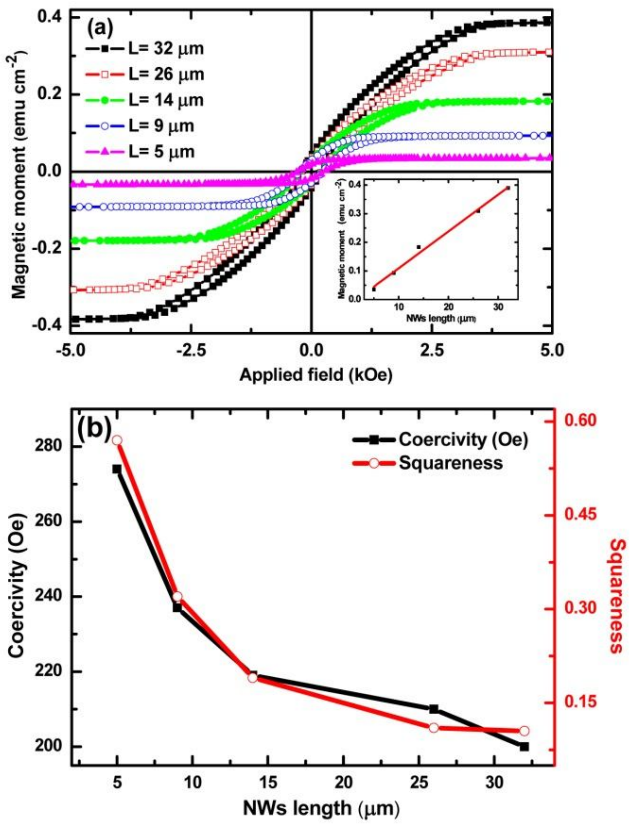

Fig. 5.(a) Out-of-plane hysteresis loops of samples with various nanowire lengths. The length dependence of saturation magnetic moment is inserted. (b) Coercivity and squareness as a function of NWs length.

In order to more precisely study the variations of magnetostatic interactions vs. length, FORC diagrams were employed. Typical FORC curves of FeCoNi nanowire arrays with the lengths of 9 and 26μm are shown in Fig. 6(f) and 6(g). In Figs. 6(a) to 6(e), FORC diagrams calculated with SF = 2 are displayed; from which a relatively large interaction field distribution in the H_u direction is observed for the longer NWs, as expected for interacting systems [21, 25]. FORC analysis revealed a linear dependence between the NWs length and magnetostatic interactions level for FeCoNiNWs.

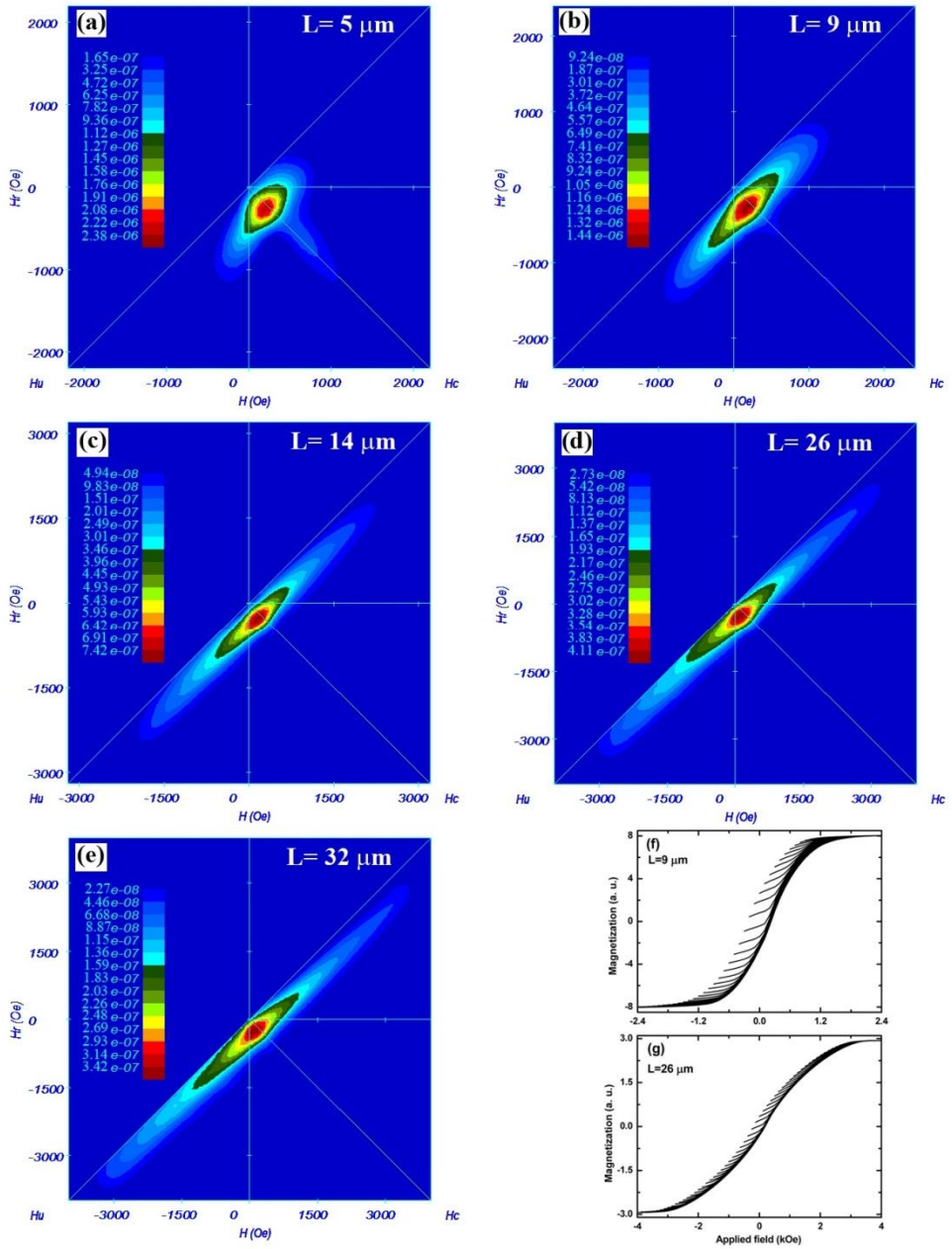

Fig. 6. Out-of-plane FORC diagrams of FeCoNi nanowire arrays with different lengths of: (a) 5, (b) 9, (c) 14, (d) 26, and (e) 32μm. Set of out-of-planeFORCs for samples with two different lengths of: (f) 9 and (g) 26μm.

A FORC diagram features two distributions: (i) interaction filed distribution (IFD), by which intrinsic coercivities of NWs within the array are obtained, and (ii) coercive field distribution (CFD), which has a large dispersion of coercivities along the *Hc* axis [30]. Simulation analyses by Dobrotă et al. indicated that the IFD is related with the FORC dependent switchings of NWs with small intrinsic coercivities whereas the CFD arises from non-uniform length distribution in the array [30]. Apart from a relatively large IFD in the H_u direction for the FeCoNi NWs with different lengths, the CFD component is observed for 5 and 9 μm long NWs. This indicates a decrease of dispersion in the length distribution with increasing the length of nanowire arrays.

On the other hand, FORC diagrams can identify the domain structure of magnetic NWs [17-20]. SD NWs have closed contours extending along the H_c axis. PSD NWs obtain oval-like contours with a peak moving towards the H_u axis. For MD NWs, the contours broaden along the H_u =0 axis. In fact, the presence of interactions produces a spreading of the distribution along the H_u axis of a FORC diagram [21, 24].

As seen in Fig. 6, with increase in the wire length, the behavior of magnetic domains changes. A transition from SD to PSD and a tendency toward MD-like due to increase in magnetostatic interaction between NWs is observed. It is known that the domain structure has its origin in the possibility of lowering the energy of a system by going from a saturated configuration with high magnetic energy to a domain configuration with a lower energy and the total magnetic energy is the sum of the anisotropy, exchange and magnetostatic energies [27, 31]. Herein, the anisotropy and exchange energies remain almost constant with increasing length of NWs; therefore the magnetostatic interactions play a predominant role in determining the domain structures. In this regard, an SD structure is observed for shorter lengths of FeCoNi NWs (see Figs. 6(a) and 6(b)). As the length increases, the role of magnetostatic interactions becomes more pronounced and the magnetostatic energy increases so that a transition from the SD to PSD structure is occurred and by minimizing the total magnetic energy, magnetic domains show MD-like behavior for the longest length (see Figs. 6(c) to 6(e)).

A quantitative method of investigating the interwiremagnetostatic interaction is to measure ΔH_u^{FORC}, which is defined as the half-width of the irreversible distribution in the $H_u$direction of out-of-plane FORC diagram. Based on the previous studies [23, 32, 33], $\Delta H_u^{FORC}$is equivalent to the interwire magnetostatic field at saturation (H_{int}^{sat}) which can be calculated by the following equation [32]:

$$H_{int}^{sat} = M_s r^2 [a(d)l + b(d)] \qquad (3)$$

where a(d) and b(d) are phenomenological functions of d (the interwire distance) which can be approximated as [32, 33]:

$$a(d) = \frac{1}{c_1 d^2 + c_2 d}, b(d) = \frac{1}{c_0} \frac{1}{c_3 d^3 + c_4 d^2 + c_5 d + 1} \quad (4)$$

The coefficients ci (i=0-5) are given in [33].

Fig.7(a) illustrates the cross-sectional view of FORC distribution, parallel to the H_u direction passing through the maximum H_c, in different lengths. The width of curves indicates distribution of magnetostatic interactions of system which enhances with increasing length. Fig. 7(b) indicates the observed changes of the half-width of the

distribution in the Hu direction (ΔH_u^{FORC}) with increasing length.Taking M_s = 1425 emu/cm^3[34], and using a linear fitting, we obtain *a(d)* = 0.66μm^{-3} which is almost the same order of the theoretically calculated value (0.59 μm^{-3}).

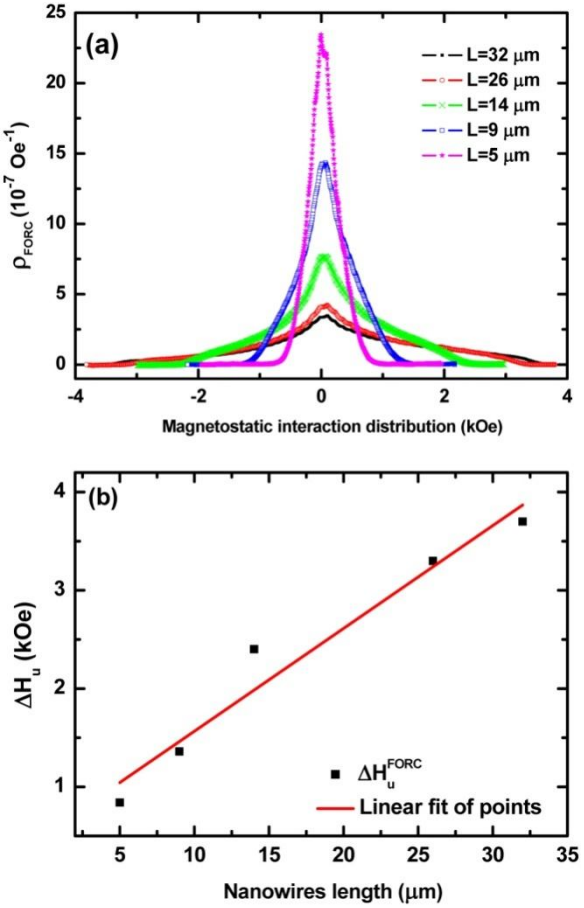

Fig. 7. (a) Magnetostatic interaction distribution for different samples. (b) Magnetostatic interaction field as a function of NWs length.

An estimation of the individual coercivity of the NWs can also be obtained from a FORC diagram.H_c^{FORC}which is H_c of irreversible peak at H_u=0; indicates unique coercivity of NWs, while H_c^{Array} is the mean coercivity of the array. A positive $\Delta(\Delta = H_c^{FORC} - H_c^{Array})$ is expected for the systems with strong interactions between NWs [24, 25]. Fig. 8(a) shows the cross-sectional view of FORC distribution along the H_c axis at H_u = 0 for different lengths of FeCoNi NWs. As the length increases, the maximum distribution tends toward a lowerH_c^{FORC}. In Fig.8(b), H_c^{FORC}, H_c^{Array} and Δ versus length are shown. There is a negative difference between the two coercivities of 5 and 9 μm longNWs. Increasing the length is accompanied with a positiveΔ.It can be said that increasing the length of NWs results in an increase inthe interaction and decrease in the array coercive field as beingsmaller than that of individual NWs.

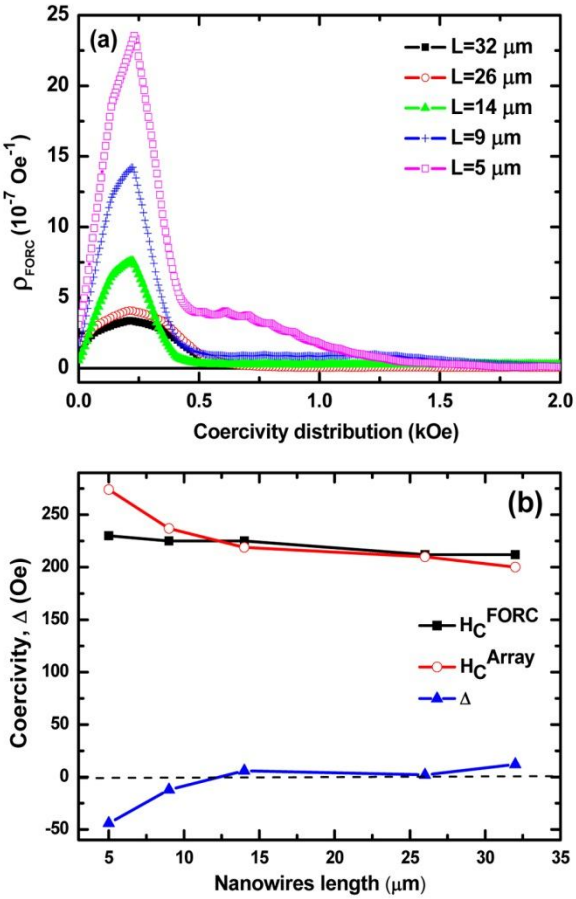

Fig. 8. (a) Coercivity distribution for different samples. (b)H_c^{FORC}, $H_c^{Array}$and Δ as a function of NWs length.

4. Conclusion

$Fe_{49}Co_{33}Ni_{18}$ nanowire arrays with the same diameter and various lengths were ac pulse electrodeposited into nanopores of HA–AAO template.Theirmagnetic properties were carefully investigated using hysteresis measurements and FORC diagrams.In agreement with the theoretical calculations, an increase in nanowire length resulted in a considerable increase in the IFD of FORC diagrams, indicating a linear correlation between the magnetostatic interactions and length of NWs. With increasing length from 5 to 32 μm, the coercivity and squareness decreased by approximately 27% and 82%, due to the enhanced magnetostatic interactions.With increasing length, a transition from SD to PSD structure and an MD-like behavior were observed. Such variations may be due to the enhanced magnetostatic interactions in longer NWs. The observed CFD component in the FORC diagrams of FeCoNi NWs with shorter lengths was a consequence ofnon-uniform length distributions.Increasing the length of NWs resulted in an increase inthe interaction and decrease in the array coercive field(H_c^{Array}) as beingsmaller than that of individual NWs (H_c^{FORC}).

Acknowledgment

The authors are grateful to the University of Kashan for providing the financial support of this work by Grant No. 159023/3.

References

[1] D. A. Allwood, G. Xiong, C. C. Faulkne, D. Atkinson, D. Petit, R. P. Cowburn, Science 309 (2005) 1688-1692.

[2] J. Sarkar, G. G. Khan,A. Basumallick, Bull. Mater. Sci. 30 (2007) 271-290.

[3] S. Shingubara, J. Nanopart. Research. 5 (2003) 17-30.

[4] W. Lee, J. Min. Met. Mater. Soc. 62 (2010) 57-63.

[5] J. Azevedo, C. T. Sousa, J. Ventura, A. Apolinario, A. Mendes, J. P. Araujo, Mater. Res. Express. 1 (2014) 015028.

[6] M. Ghaffari, A. Ramazani, M. Almasi Kashi, J. Phys. D: Appl. Phys. 46 (2013) 295002.

[7] A. Ramazani, M. Almasi Kashi, G. Seyedi, J. Magn. Magn. Mater. 324 (2012) 1826-1831.

[8] M. Albrecht, G. Hu, A. Moser, B. D. Terris, J. Appl. Phys. 97 (2005) 103910-5.

[9] T. C. Arnoldussen, L. L. Nunnelley, Noise in Digital Magnetic Recording. Singapore: World Scientific, 1992.

[10] W. Lee, R. Ji, U. Gösele, K. Nielsch, Nat. Mater. 5 (2006) 741-747.

[11] H. Masuda, K. Fukuda, Science 268 (1995) 1466-1468.

[12] M Fearon, R. W. Chantrell,E. P. Wohlfarth, J. Magn. Magn. Mater. 86 (1990) 197-206.

[13]M. Walker P. I. Mayo, K. O'Grady, S. W. Charles,R. W. Chantrell, J. Phys: Condens. Matter 5 (1993) 2793-2808.

[14]X-d. Che, H. Neal Bertram, J. Magn. Magn. Mater. 116 (1992) 121-127.

[15] M. P. Proenca, K. Merazzo, L. Vivas, D. Leitao, C. Sousa, J. Ventura, J. Araujo, M. Vazquez, Nanotechnology 24 (2013) 475703.

[16] A. P. Roberts, C. R. Pike, K. L. Verosub, J. Geophys. Res. 105 (2000) 28461-28475.

[17] R. Leonhardt, D. Krása, R. S. Coe, phys. earth. planet. in. 147 (2004) 127-140.

[18] C. Carvallo, A. R. Muxworthy, D. J. Dunlop, W. Williams, Earth Planet. Sci. Lett. 213 (2003) 375-390.

[19] A. R. Muxworthy, D. J. Dunlop, Earth Planet. Sci. Lett. 203 (2002) 369-382.

[20] C. R. Pike, A. P. Roberts, M. J. Dekkers, K. L. Verosub, phys. earth. planet. in. 126 (2001) 11-25.

[21]M. Almasi Kashi, A. Ramazani,A. Esmaeily, IEEE Trans. Magn. 49 (2013) 1167-1171.
[22]Y. P. Ivanov, M. Vázquez, O. Chubykalo-Fesenko, J. Phys. D: Appl. Phys. 46 (2013) 485001.
[23] F. Béron, L. Clime, M. Ciureanu, D. Ménard, R. W. Cochrane, A. Yelon, J. Nanosci. Nanotechnol. 8 (2007) 1-11.
[24] S. Samanifar, M. Almasi Kashi, A. Ramazani and M. Alikhani, J. Magn. Magn. Mater. 378 (2015) 73-83.
[25] S. Alikhanzadeh Arani, M. Almasi Kashi, A. Ramazani, Curr. Appl. Phys. 13 (2013) 664-669.
[26] W. D. Zhong, Ferromagnetism, Beijing: Science Press, 1998.
[27] B. D. Cullity, C. D. Graham, Introduction to magnetic materials, John Wiley & Sons, 2008.
[28] L. Sun, Y. Hao, C-L. Chien, P. C. Searson IBM J. Res. Dev. 49 (2005) 79-102.
[29] G. C. Han, B. Y. Zong, P. Luo, Y. H. Wu, J. Appl. Phys. 93 (2003) 9202-9206.
[30] C-I. Dobrotă, A. Stancu, J. Appl. Phys. 113 (2013) 043928.
[31] C. Kittel, P. McEuen, Introduction to solid state physics, Academic, New York: Wiley, 1980.
[32] M. Ciureanu, F. Béron, P. Ciureanu, R. W. Cochrane, D. Ménard, A. Sklyuyev, A. Yelon, J. Nanosci. Nanotechnol. 8 (2008) 5725-5732.
[33] L. Clime, F. Béron, P. Ciureanu, M. Ciureanu, R. W. Cochrane,A. Yelon, J. Magn. Magn. Mater. 299 (2006) 487-491.
[34] L. Comstock, Magnetic Information-Storage Materials,Springer Handbook of Electronic and Photonic Materials, 2007.